Geochemical Journal, Vol. 36, pp. 527 to 543, 2002

Controls on the REE tetrad effect in granites: Evidence from the Qianlishan and Baerzhe Granites, China

ZHAO ZHENHUA,[1]* XIONG XIAOLIN,[1] HAN XIAODONG,[1] WANG YIXIAN,[1] WANG QIANG,[1] BAO ZHIWEI[1] and BORMING JAHN[2]

[1]Guangzhou Institute of Geochemistry, Chinese Academy of Sciences, Guangzhou 510640,China
[2]Geosciences Rennes, Universitė de Rennes 1, 35042 Rennes Cedex, France

(*Received September 13, 2001; Accepted May 27, 2002*)

REE contents in whole-rock samples and constituent minerals of the Qianlishan and Baerzhe granites from China were determined using three analytical methods (ICP-AES, ICP-MS, and ID-TIMS). The REE abundance patterns of the granites show the M-type tetrad effect and strong Eu depletion in both whole-rock samples and in individual minerals samples. Fluid-melt interaction in the late stage of fractional crystallization is suggested to be the most important factor controlling the formation of REE tetrad effects in the granites.

INTRODUCTION

The REE tetrad effect was first found by Peppard *et al*. (1969) in an experiment of REE partitioning in a pure chemical liquid-liquid extraction system. The distribution pattern shows four distinct sectors (La-Ce-Pr-Nd, Pm-Sm-Eu-Gd, Gd-Tb-Dy-Ho, Er-Tm-Yb-Lu) separated at three positions corresponding to (1) between Nd an Pm, (2) at Gd, and (3) between Ho and Er. Since then, a number of studies demonstrated that some physical properties of REE, such as ionic radius, unit cell volume and free energy of formation of complex, possess the characteristic feature of tetrad effect. Nugent (1970) and Siekierski (1971) considered the REE tetrad effect to be related to 4f electron shell of Ln^{3+}, and Jørgenson (1962, 1979), Kawabe (1992) interpreted the REE tetrad effect in terms of a refined spin-pairing energy theory (RSPET). Masuda *et al*. (1994) proposed a mathematicall method to express the comparative degree of the tetrad effect numerically.

In most geological samples the chondrite-normalized REE abundances form a smooth linear or curvilinear trend, which is the famous Masuda-Coryell diagram (Henderson, 1984; Rollison, 1993). Consquently, some ratios, such as $(La/Yb)_N$, $(La/Sm)_N$, $(Gd/Yb)_N$ and Eu/Eu*, Ce/Ce* can provide important petrogenetic and metallogenic information (Schi1ling, 1975; Jahn *et al*., 1982; Frey, 1984; Rollison, 1993). In the last 20 years, many precisely determined REE data, by ID, ICP-MS or ICP-AES showed that the chondride-normalized REE patterns of rocks formed in special conditions do not show smooth lines or curves. Instead, they constitute four sectors of curves identical to the tetrad effect produced in two-liquid chemical system. Masuda and Ikeuchi (1979) first found the W-type REE tetrad effect in various marine materials, including seawater, algae, sponges, shells limestones, etc., and soon afterwards, they found similar REE distribution feature in groundwater. Masuda *et al*. (1987) and Zhao, Z. H. (1988, 1992) found the M-type REE tetrad effect in rare-metal granites of South China. Bau (1996) and Irber (1999) also found the same feature in granites of Egypt and Germany. In recent years, many geological sam-

*Corresponding author (e-mail: zhzhao@gig.ac.cn)

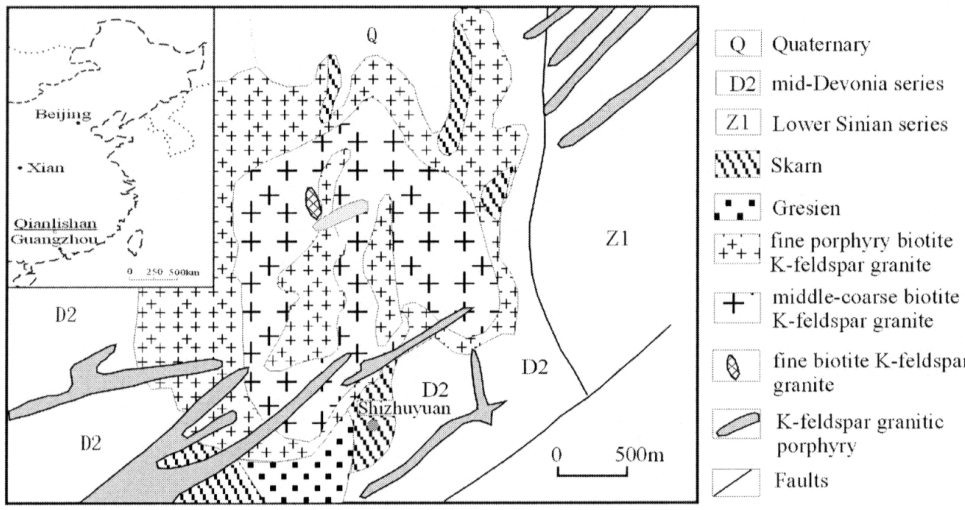

Fig. 1. Geological sketch map of the Qianlishan granite complex (after Zhao Y. X., 1988, with minor revision).

ples, including pegmatite (Jolliff *et al.*, 1989; Yurimoto *et al.*, 1990), uraninite (Hidaka *et al.*, 1992), kimuraite (Akagi *et al.*, 1993) and clastic sediments (Liu *et al.*, 1993) were reported to show the REE tetrad effect. It appears that such REE tetrad effect is a record of special petrogenetic and metallogenetic process. It revises and complements the linear trend in Masuda-Coreyll diagram and can be used as an important tracer in petrogenetic and metallogenic investigations.

The REE tetrad effect is a new frontier of geochemistry. Since the discovery of REE tetrad effect in granites of South China in 1987, we have devoted our study to its formation mechanism. In this paper we report high precision REE data for whole-rock samples and constituent minerals for the Qianlishan and Baerzhe granites. We demonstrate the presence of the tetrad effects not only in whole-rock samples but also in the constituent minerals. We will argue that interaction between granitic melt and F, Cl-rich fluid was the most important mechanism for the formation of REE tetrad effect. The Qianlishan and Baerzhe granites are closely associated with the superlarge (giant) W-Bi deposit and REE-Nb-Zr-Be deposit, respectively. The investigation of the formation mechanism of REE tetrad effect will contribute to a better understanding of the genesis of the related superlarge ore deposits.

Sample Description

The Qianlishan K-feldspar granite pluton is located about 15 km SE of Chenzhou city in Southern Hunan Province. It's outcrops are about 9.8 km^2 (Fig. 1). The famous superlarge W-Bi deposit in Shizhuyuan is closely associated with it in space and genesis. Lithologically, it comprises fine-grained porphyritic biotite K-feldspar granite, medium to coarse-grained biotite K-feldspar granite, fine to coarse-grained biotite K-feldspar granite and K-feldspar granitic porphyry. Their ^{40}Ar-^{39}Ar ages are in the range of 144–183 Ma (Liu *et al.*, 1997). The principal mineralogical phases are microcline, oligoclase (An = 11–18), quartz and biotite, and accessory minerals are monazite, zircon, thorite and topaz, etc. The granites have a high-SiO_2 (74–75 wt%) and high-alkali (K_2O + Na_2O = 8–8.4 wt%) contents and are volatile-rich (F 3200–9900 ppm, Cl 220–500 ppm, B 20–72 ppm) (Table 1) (Liu *et al.*, 1996; Mao *et al.*, 1995).

The Baerzhe riebeckite granite is situated in Jarud Qi, Inner-Mongolia Autonomous Region. It's outcrops are about 0.24 km^2 (Fig. 2). The gran-

Table 1. Chemical compositions (%) of the Qianlishan and Baerzhe granites (F, Cl, B in ppm)

No.	SiO_2	TiO_2	Al_2O_3	Fe_2O_3	FeO	MnO	MgO	CaO	Na_2O	K_2O	P_2O_5	H_2O^+	F	Cl	B
Qianlishan granite															
R_5^{2b-1}	74.68	0.17	12.42	0.72	1.43	0.03	0.18	1.18	3.44	4.61	0.04	0.68	3295	333	67.5
R_5^{2b-2}	75.26	0.06	12.64	0.35	1.37	0.04	0.15	0.76	3.72	4.19	0.03	0.63	3498	504	72.3
R_5^{2c}	74.96	0.04	13.41	0.37	0.88	0.28	0.28	0.50	3.91	4.50	0.02	0.52	9899	299	60.00
R_5^{2d}	74.07	0.20	12.49	0.63	1.59	0.30	0.30	1.16	2.81	5.25	0.04	0.87	3251	220	20
Baerzhe granite															
Ba-6	73.75	0.68	9.05	4.20		0.15	0.00	0.06	2.71	3.81	0.05	0.47*	190		
Ba-8	70.48	0.75	9.83	5.42		0.12	0.03	0.09	3.59	3.46	0.03	0.74*	270		
Ba-11	72.24	0.71	9.63	4.75		0.15	0.00	0.04	3.65	3.71	0.03	0.40*	920		
Ba-12	74.02	0.25	11.02	3.64		0.11	0.03	0.05	4.02	4.50	0.02	0.57*	940		
Ba-14	71.88	0.68	12.04	3.18		0.24	0.00	0.05	4.15	4.68	0.02	0.40*	410		
Ba-16	74.95	0.19	10.87	3.42		0.13	0.02	0.09	3.96	4.12	0.02	0.60*	800		
B-19	74.26	0.23	10.94	4.07		0.12	0.00	0.17	3.78	4.80	0.02	0.37*	1250		—
B-22	74.77	0.26	10.95	3.61		0.19	0.01	0.10	4.11	4.43	0.02	0.35*	1040		—
B-27	74.93	0.16	11.12	3.26		0.09	0.00	0.20	4.13	4.66	0.02	0.22*	1900		—
B-30	73.80	0.15	11.62	3.87		0.16	0.01	0.29	4.55	4.57	0.01	0.36*	1850		—
Ba-43	73.93	0.17	9.73	6.23		0.20	0.00	0.06	3.55	5.02	0.03	0.43*	2500		
Ba-44	74.16	0.15	9.81	5.39		0.09	0.01	0.05	4.00	4.90	0.04	0.41*	860		
Ba-47	73.83	0.17	10.03	5.56		0.11	0.00	0.06	4.25	4.55	0.02	0.30*	1350		
Ba-50	74.04	0.14	9.51	6.13		0.13	0.00	0.08	4.49	3.61	0.02	0.70*	730		

*R_5^{2b-1}: fine porphyry biotite K-feldspar granite; R_5^{2b-2}: middle-coarse biotite K-feldspar granite; R_5^{2c}: fine biotite K-feldspar granite; R_5^{2d}: K-feldspar granitic porphyry; Ba-6–Ba-50: riebeckite granite; *LOI.*

ite is closely associated with a REE-Nb-Be-Zr superlarge deposit (located in top of the pluton). The Rb-Sr isochron age of whole rock is 122 ± 5 Ma (Wang and Zhao, 1997). The rock-forming minerals are microcline-perthite, albite, quartz, riebeckite and rarely aegirine, and accessory minerals include hingganite, pyrochlore, monazite, zircon and columbite, etc. High SiO_2 (73–75 wt%), low Al_2O_3 (10–12 wt%), high alkali (K_2O + Na_2O = 8.6–9.1 wt%) and high F contents (F 190–2500 ppm) are the distinct characteristics of this granites (Table 1).

Mineral separation was achieved using an oscillating table, a heavy liquid and a Frantz magnetic separator. Individual minerals were purified to ~100% using hand-picking under a binocular microscope. Feldspar, biotite, monazite and topaz were separated from a medium to coarse-grained biotite K-feldspar granite (S94-1) of the Qianlishan granite; microcline, riebeckite, hingganite and pyrochlore were separated from the Baerzhe granite (Ba-19).

Analytical Methods

The REE contents were measured using inductively-coupled atomic emission spectrometry (ICP-AES) and inductively-coupled mass spectrometry (ICP-MS). About 50 mg sample powder was dissolved using HF/HNO_3 (10:1) mixture in screw-top teflon beakers for 7 days at ~100°C, followed by evaporation to incipient dryness, refluxing in 7N HNO_3 to incipient dryness again, and then dissolving the sample cake in 2% HNO_3. An international standard solution containing Rh was then added and the spiked sample solutions were diluted with 2% HNO_3 to a sample/solution weight ratio of 1/1000. USGS standard BCR-1 was chosen for calibration of element concentration of measured samples. Two USGS standards—BHVO-1 and W-2 were analysed in this study. Table 2 lists the results analysed with ICP-MS and the standard deviation. It is clear that our results are in good agreement with the compiled values.

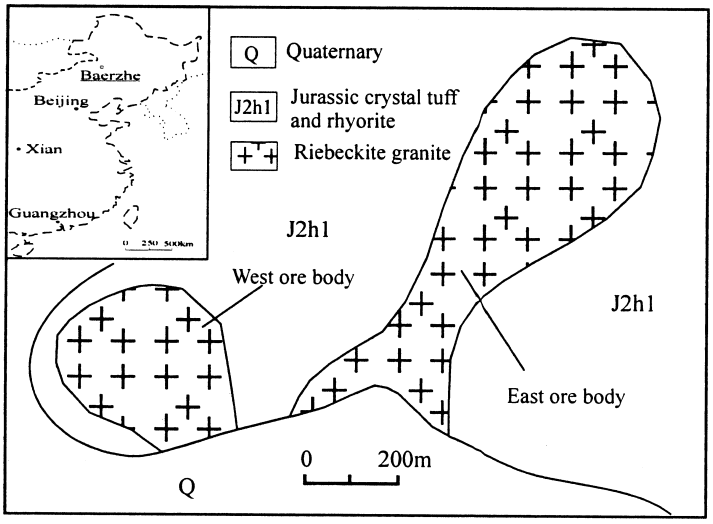

Fig. 2. Geological sketch map of the Baerzhe granites.

Table 2. REE concentrations (ppm), precision and compiled values for USGS reference materials of BHVO-1 and W-2, including calibration values for BCR-1

Element	BCR-1	BHVO-1			W-2		
	Calibration values	Mean (n = 4)	Standard deviation	Compiled values	Mean (n = 7)	Standard deviation	Compiled values
La	24.9	15.9	1.0	15.8	10.7	0.3	11.4
Ce	53.7	40.6	1.4	39	23.7	0.5	24
Pr	6.8	5.6	0.2	5.7	2.95	0.07	(5.9)
Nd	28.8	25.6	0.9	25.2	12.7	0.4	14
Sm	6.59	6.4	0.2	6.2	3.21	0.07	3.25
Eu	1.95	2.1	0.12	2.06	1.06	0.03	1.1
Gd	6.68	6.3	0.2	6.4	3.55	0.12	3.6
Tb	1.05	0.96	0.02	0.96	0.59	0.03	0.63
Dy	6.34	6.4	0.2	5.2	3.66	0.13	3.8
Ho	1.26	0.97	0.05	0.99	0.74	0.03	0.76
Er	3.63	2.6	0.1	2.4	2.13	0.07	2.5
Tm	0.56	0.34	0.04	0.33	0.32	0.02	0.38
Yb	3.38	2.11	0.09	2.02	2.00	0.09	2.05
Lu	0.51	0.296	0.01	0.291	0.30	0.01	0.33

Calibration values for BCR-1 and compiled values for BHVO-1 and W-2 were from Govindaraju (1994). The REE concentrations were determined using ICP-MS.

In this paper we also performed an inter-laboratary check and evaluated the analytical precision between ICP-AES, ICP-MS and ID-TIMS (isotopic dilution mass spectrometry), the later is considered as the most accurate method for REE analysis. Using ICP-AES, ICP-MS and ID-TIMS the same sample Ba-30 was analysed (Table 3, Fig. 7). respectively. The samples, such as Ba-6, Ba-8, Ba-14, Ba-16, Ba-22, and Ba-30, were analysed with both ICP-AES and ID-TIMS (Table 3, Figs. 4a, 4b, 7). The ID-TIMS analysis was carried out in the geochemical laboratary at Universite de Rennes. Table 3 lists the comparison of the analytical results. Four mono-isotopic elements of

Table 3. Comparisons of REE contents (ppm) of the Baerzhe granites analyzed with ICP-AES, ICP-MS and ID-TIMS

	Ba-6			Ba-8			Ba-14		
	ICP-AES	ID-TIMS	RD (%)	ICP-AES	ID-TIMS	RD (%)	ICP-AES	ID-TIMS	RD (%)
La	425	430.2	–1.2	405	377	7.5	225	218.3	3.2
Ce	1139	1182	–3.6	1005	1094	–8.2	739	758	–2.5
Pr	146	—		131	—		84	—	
Nd	517	530.9	–2.7	479	510.2	–6.1	291	296.8	–2
Sm	159	169.2	–6	153	172.4	–11.2	87	89	–2
Eu	1.98	1.45	26.9	1.95	1.53	21.5	1.11	0.783	41.8
Gd	160	168.2	–4.9	155	195	–20.7	83.3	84.7	–1.7
Tb	35	—		34.3	—		17.3	—	
Dy	235	247	–4.5	228	253.2	–10	113	115.2	–2
Ho	46.5	—	—	44.3	—		22.6	—	
Er	147	163.7	–10.2	131	149.9	–14.1	72.7	74	–1.8
Tm	24.5	—		20.5	—		12.2	—	
Yb	158	173.2	–8.9	124	136.5	–9.1	79.1	76.2	3.8
Lu	22.8	24.11	–5.4	17.8	17.8	0.2	11.9	10.6	12.3

	Ba-16			Ba-22			Ba-30				
	ICP-AES	ID-TIMS	RD (%)	ICP-AES	ID-TIMS	RD (%)	ICP-AES	ICP-MS	ID-TIMS	RD (%)	RD (%)*
La	158.1	147.4	7.3	110	107.4	2.8	57.6	56.8	57.38	0.4	–1
Ce	425.4	430.2	–1.1	268	279.1	–0.4	138	149	154.1	–10.5	–3.2
Pr	55.6	—		32.8	—		17.7	18.8	—		
Nd	216.1	214	1	116	120.1	–3.6	66.1	68.4	71.33	–7.3	–4.1
Sm	63.3	64.3	–1.6	30.9	32.6	–5.2	17.3	17.8	18.72	–7.6	–4.8
Eu	0.81	0.565	43.3	0.45	0.337	33.5	0.25	0.21	0.206	21.4	1.9
Gd	62	62.6	–1	28.6	37	–22.7	16.1	18.9	20.3	–20.7	–6.9
Tb	11.5	—		5.9	—		3.1	3.04			
Dy	65.8	65.9	–0.2	35.8	39.07	–0.4	18.7	21.7	20.1	–7	1.2
Ho	12.1	—		6.9	—		3.6	4.1			
Er	32	32.54	–1.7	20.6	20.52	0.4	10.9	12.3	11.7	–6.8	–4.8
Tm	4.5	—		3.3	—		1.8	1.83	—		
Yb	27.6	24.68	11.8	22	17.68	24.4	11.5	11.91	11.34	1.4	5
Lu	3.9	3.28	19	3.1	2.42	28.4	1.6	1.69	1.609	–0.6	5.6

RD: Relative Deviation of ICP-AES vs. ID-TIMS.
RD: Relative Deviation of ICP-MS vs. ID-TIMS.*

REE (Pr, Tb, Ho and Tm) cannot be analysed by ID-TIMS. The results of other ten elements are in good agreement within the analytical errors with that of ICP-AES and ICP-MS. The results of ICP-AES and ICP-MS methods are systematically slightly lower than that of ID-TIMS. For the ICP-AES the relative errors less than 10%, except for Eu due to its very low contents. For the ICP-MS the relative errors less than or nearly to 5%.

RESULTS

The analytical results of REE contents of whole rocks and separated minerals are listed in Tables 4–6, and the chondrite-normalized REE patterns are shown in Figs. 3–6 (chondrite values were from Boynton, 1984, Table 4).

There is a close resemblance of REE abundance patterns between the Qianlishan and

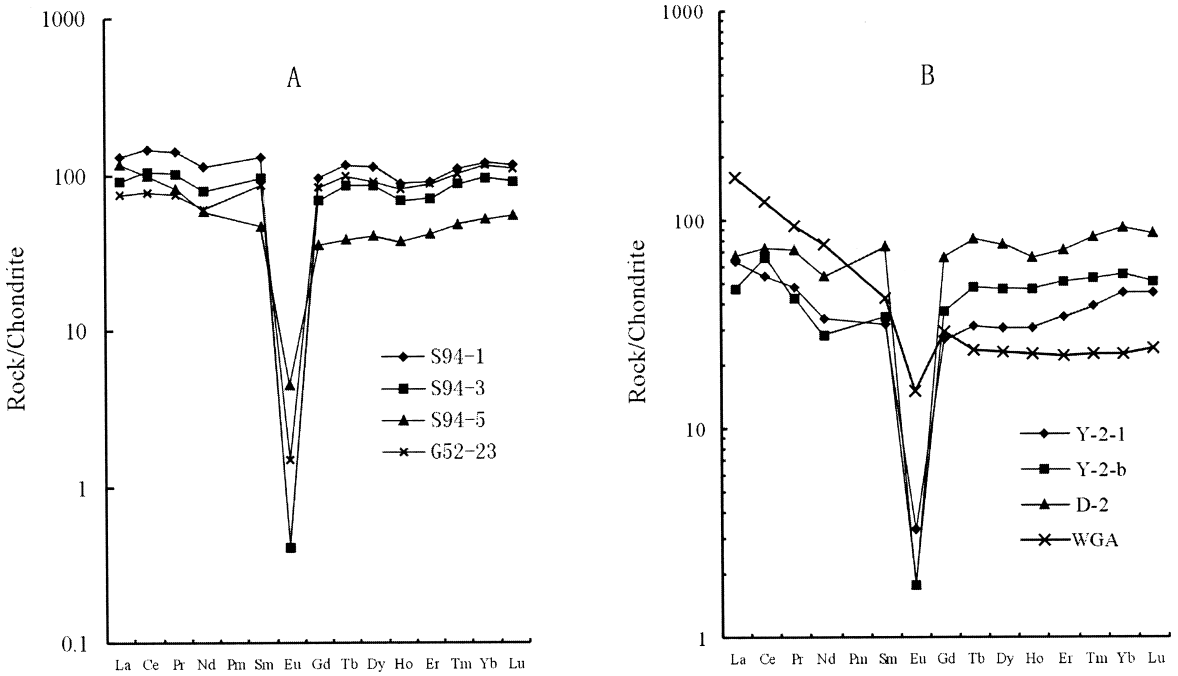

Fig. 3. REE abundance patterns of the Qianlishan granites. Numbers of the legends are referred to Table 4. The WGA represents the average of 213 granites (SiO_2 > 70%) in the world (Haskin and Haskin, 1968).

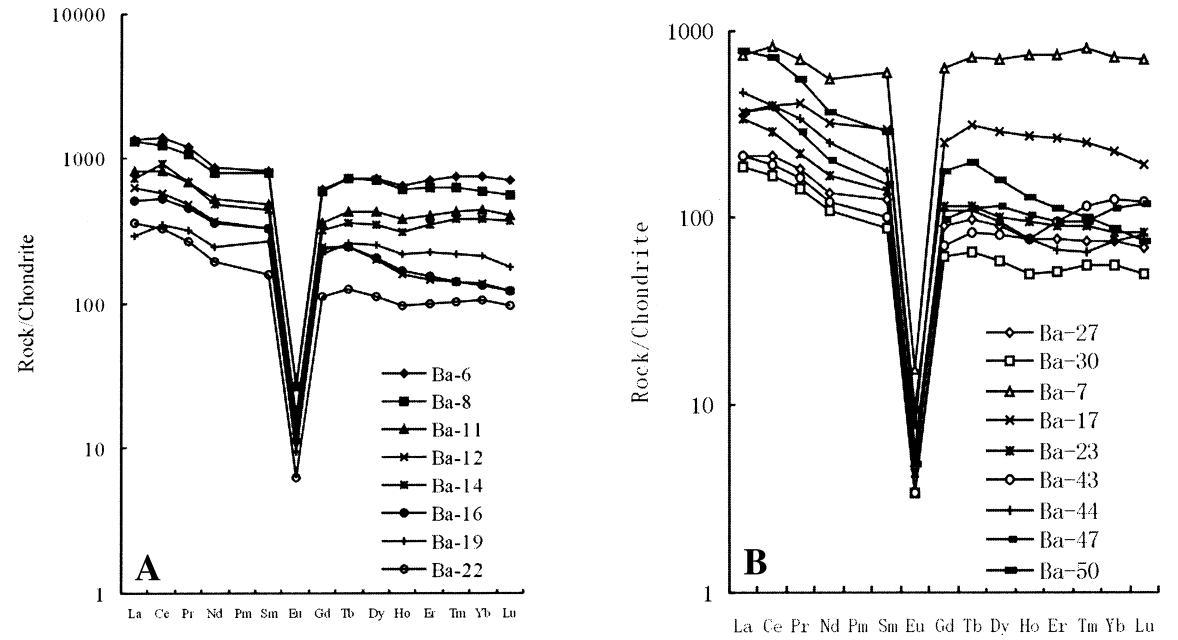

Fig. 4. REE abundance patterns of the Baerzhe granites. Numbers of the legends are referred to Table 5. Analysed with ICP-AES: Ba-6, 8, 11, 12, 14, 16, 19, 22, 27, 30, 43, 44, 47, 50. Analysed with ICP-MS: Ba-7, 17, 23, 30.

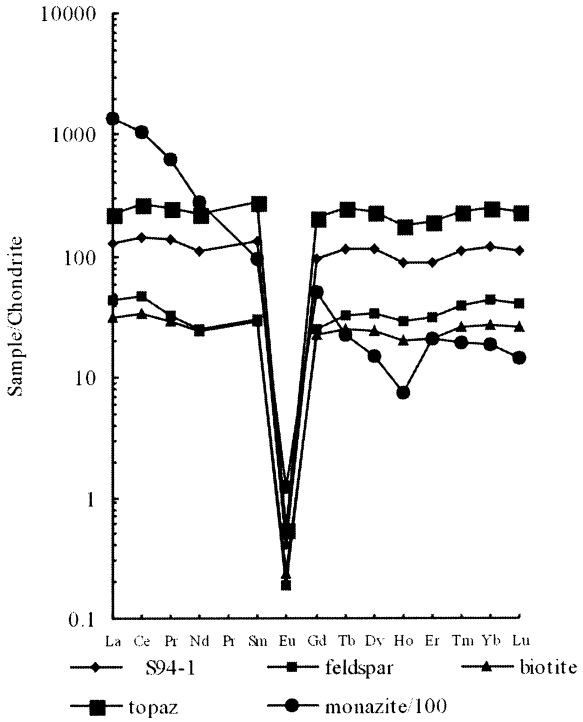

Fig. 5. REE abundance patterns of minerals of the Qianlishan granites.

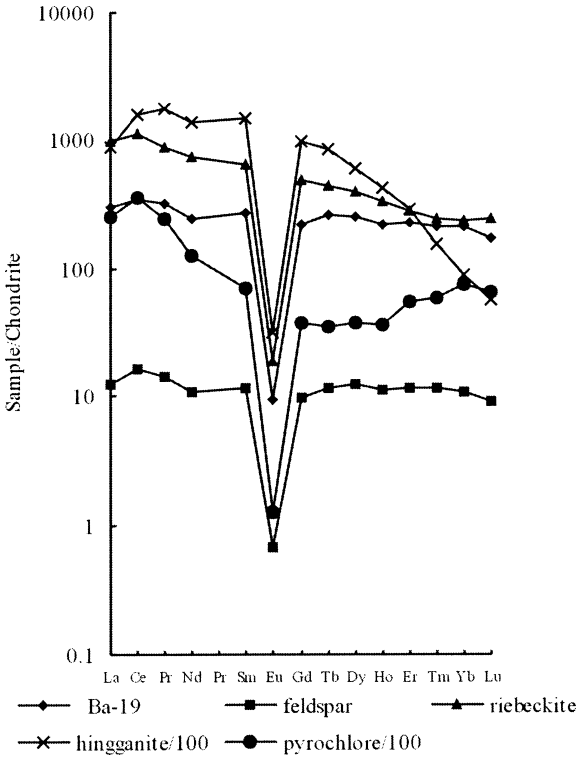

Fig. 6. REE abundance patterns of minerals of the Baerzhe granites.

Baerzhe granites. Both of them show clearly tetrad effect and possess high total REE abundances (∑REE 201–566 ppm and 465–4392 ppm, respectively), strong Eu depletion (Eu/Eu*: 0.004–0.11 and 0.044–0.38, respectively) and relative enrichment of heavy REE $(La/Yb)_N$: 0.65–2.2 and 1.4–3.3, respectively. The M-type REE tetrad effect is clearly visible in the Qianlishan and Baerzhe granites. Due to the strong depletion, Eu in the second tetrad (Pm-Sm-Eu-Gd) deviates from M-type pattern (Figs. 3 and 4).

Using the quantification method proposed by Irber (1999) the degree of REE tetrad effect for the Qianlishan and Baerzhe granites were calculated. The TE_1 and TE_3 represent the tetrad effect of the first and the third group of REE respectively (Tables 4 and 5).

The characteristic features of REE abundance patterns for the separated minerals are very similar to those of whole-rocks (Figs. 5 and 6). Feldspar, biotite and topaz of the Qianlishan granites demonstrate strong Eu depletion (Eu/Eu* = 0.002–0.009) and relative enrichment of heavy REE $(La/Yb)_N$ = 0.9–1.1. All of their REE abundance patterns are of obvious M-type tetrad effects (Fig. 5). Monazite of the Qianlishan granites possesses more fractionated REE distribution with $(La/Yb)_N$ = 73.3. Nevertheless it still possesses strong Eu depletion and obvious M-type REE tetrad effect.

The separated minerals of the Baerzhe granite also display similar REE distribution characteristics to their whole-rock. Microcline, riebeckite, hingganite ($(Y,Yb)BeSiO_4(OH)$) and pyrochlore ($(Ca,Na)_2Nb_2O_6(OH,F)_2$) are all strongly depleted in Eu (Eu/Eu* = 0.026–0.057) and show obvious M-type REE tetrad effects. Hingganite and pyrochlore are REE-enriched accessory minerals and their light REE contents are 3–7 times higher

Table 4. REE contents of the Qianlishan granites (ppm)[4)]

Sample	S94-1	S94-3	S94-5	G52-23	Y-2-1	Y-2-b	D-2	SGA[1)]	WGA[2)]	Chondrite[3)]
La	40.5	28.3	36.0	23.2	19.8	14.5	20.8	40.8	50	0.310
Ce	116	85.1	79.2	62.7	43.9	53.9	59.4	79.6	100	0.808
Pr	17.2	12.3	9.94	9.11	5.82	5.11	8.78	9.15	11.4	0.122
Nd	67.2	48.1	35.5	36.4	20.2	16.7	32.5	30.9	46	0.600
Sm	25.7	18.8	9.03	17.0	6.13	6.66	14.7	6.52	8.3	0.195
Eu	0.03	0.03	0.33	0.11	0.24	0.13	0.13	0.87	1.1	0.0735
Gd	24.8	18.0	9.11	21.8	6.89	9.55	17.3	6.12	7.6	0.259
Tb	5.45	4.1	1.83	4.7	1.48	2.24	3.87	1.06	1.12	0.0474
Dy	36.5	27.9	13.3	29.4	9.84	15.2	24.8	5.41		0.322
Ho	6.42	4.98	2.7	5.85	2.20	3.33	4.78	1.09	1.62	0.0718
Er	19.0	14.9	8.72	18.6	7.17	10.6	15.2	2.96	4.70	0.210
Tm	3.57	2.86	1.58	3.29	1.27	1.71	2.67	0.54	0.74	0.0324
Yb	24.7	20.0	11.0	24.1	9.28	11.6	19.2	2.91	4.80	0.209
Lu	3.72	2.96	1.79	3.55	1.43	1.64	2.77	0.52	0.78	0.0322
Y	176	133	97.7	185	65.7	95.4	156	30.1	42	
∑REE	567	421	318	445	201	249	383	219	280	
Eu/Eu*	0.004	0.005	0.111	0.018	0.11	0.049	0.02	0.46	0.42	
$(La/Yb)_N$	1.10	0.96	2.20	0.65	1.44	0.84	0.64	9.44	7.02	
Rb	598	759	547	830	642	778				
K/Rb	64	46	80	43	59	50				
TE_1[5)]	1.175	1.206	1.078	1.13	1.098	1.465	1.207	1.045	0.967	
TE_3[5)]	1.232	1.247	1.097	1.15	1.082	1.142	1.19	1.023		

[1)]Average of 52 biotite monzonite granites, from Zhao Zhenhua (1992).
[2)]Average of 213 granites (SiO_2>70%), from Haskin and Haskin (1968).
[3)]From Boynton (1984).
[4)]REE contents of all the samples are measured with ICP-AES.
[5)]$TE_1 = (Ce_N/(La_N^{2/3} \times Nd_N^{1/3}) \times Pr_N/(La_N^{1/3} \times Nd_N^{2/3}))^{1/2}$, $TE_3 = (Tb_N/(Gd_N^{2/3} \times Ho_N^{1/3}) \times Dy_N/(Gd_N^{1/3} \times Ho_N^{2/3}))^{1/2}$, from Irber (1999).

than the whole-rock.

Using $REE_{miner.}/REE_{wr.}$ the apparent partition coefficients (K_d) of REE were calculated for all the separated minerals (Table 7). It is clear that the K_d values of Eu for feldspars of the Qianlishan and Baerzhe granites are both higher than other REE but much lower (<1.0) than the published value in the literatures (>1.0).

DISCUSSION

(1) The tetrad effects are resulting from genuine natural fractionation processes but not from analytical uncertainties

Mclennan (1994) attributed the tetrad effect of REE abundance patterns in geological samples to the result of analytical uncertainties. The results of our analyses using different analytical methods (ICP-AES, ICP-MS and ID-TIMS) are comparable (Table 3) and have all shown clearly tetrad effect. For example we get a same tetrad effect for the sample No. Ba-30 of the Baerzhe granite using ICP-AES, ICP-MS and ID-TIMS methods (Table 3, Fig. 7). These results suggest that the "irregular" REE patterns are not due to analytical problems, rather, they represent the tetrad effect (Figs. 3–7).

(2) REE tetrad effect of granites exhibits the integrated contributions of their constituent minerals

a) REE tetrad effects have been reported for a number of highly evolved granitic rocks including leucogranites and pegmatite (Walker *et al.*, 1986; Masuda *et al.*, 1987; Zhao, Z. H., 1988; Zhao *et al.*, 1992; Jolliff *et al.*, 1989; Yurimoto *et al.*, 1990; McLennan, 1994; Irber, 1999). Some

Table 5. REE compositions (ppm) of the Baerzhe riebeckite granites analysed with ICP-AES and ICP-MS

	Ba-6	Ba-8	Ba-11	Ba-12	Ba-14	Ba-16	Ba-19	Ba-22	Ba-27
La	425	405	253	198	225	158	92.0	110	66.8
Ce	1139	1005	655	467	739	425	280	268	176
Pr	146	1301	84.5	59.4	84.0	55.6	39.0	32.8	22.3
Nd	517	479	316	225	291	216	149	116	82.2
Sm	159	153	94.8	63.9	87.2	63.3	53.0	30.9	24.1
Eu	1.98	1.95	1.22	0.87	1.11	0.81	0.68	0.45	0.34
Gd	160	155	93.3	63.9	83.3	62.0	57.0	28.6	23.6
Tb	35.0	34.3	20.6	11.6	17.3	11.5	12.4	5.9	4.7
Dy	235	228	138	64.7	113	65.8	82.3	35.8	28.9
Ho	46.5	44.3	27.5	11.3	22.6	12.1	15.7	6.9	5.6
Er	147	131	85.2	30.1	72.7	32.0	47.6	20.6	16.0
Tm	24.5	20.5	13.8	4.5	12.2	4.5	7.0	3.3	2.4
Yb	158	124	93.3	28.8	79.1	27.6	44.4	22.0	15.5
Lu	22.8	17.8	13.2	3.9	11.9	3.9	5.7	3.1	2.2
Y	1175	1091	691	293.7	627	364	435	187	156
Σ	4392	4020	2581	1526	2466	1504	1321	871	626
Eu/Eu*	0.038	0.039	0.060	0.042	0.040	0.040	0.038	0.046	0.044
(La/Yb)	1.81	2.19	1.82	4.60	1.91	3.84	1.39	3.36	2.88
Rb	1366	1346	1051	941	1132	920	912	511	560
K/Rb	23	21	29	40	34	39	44	72	69
TE_1	1.20	1.13	1.14	1.0	1.33	1.14	1.23	1.14	1.16
TE_3	1.16	1.18	1.16	1.13	1.12	1.11	1.18	1.14	1.17
Method	ICP-AES	ICP-AES	ICP-AES	ICP-AES	ICP-AES	ICP-AES	ICP-AES	ICP-AES	ICP-AES

	Ba-43	Ba-44	Ba-47	Ba-50	Ba-30	Ba-30	Ba-7	Ba-17	Ba-23
La	66.4	147	113	243	57.6	56.8	232	115	105
Ce	155	323	31	578	138	148	660	327	233
Pr	19.8	41.0	34.8	68.1	17.7	18.8	86.1	49.5	27.0
Nd	72.8	151	123	220	66.1	68.4	328	195	102
Sm	19.9	34.9	29.7	55.7	17.3	17.8	116	58.0	26.9
Eu	0.25	0.41	0.35	0.69	0.25	0.21	1.12	0.55	0.313
Gd	18.5	28.1	25.3	46.3	16.1	18.9	165	65.4	30.1
Tb	4.0	5.2	5.3	9.4	3.1	3.0	34.3	15.0	5.52
Dy	26.5	30.4	37.0	51.6	18.7	21.7	225	92.9	32.2
Ho	5.5	5.5	7.5	9.2	3.6	4.1	53.3	19.5	6.87
Er	20.1	14.0	19.9	23.8	10.9	12.3	156	55.6	19.0
Tm	3.7	2.1	3.1	3.3	1.8	1.83	26.1	8.13	2.93
Yb	26.2	15.7	23.8	18.5	11.5	11.9	153	47.1	17.2
Lu	3.9	2.6	3.8	2.4	1.6	1.69	22.8	6.18	2.68
Y	186	148	198	264	101	113	1283	571	182
Σ	628	948	940	1594	465	498	3542	1607	793
Eu/Eu*	0.040	0.040	0.039	0.042	0.046	0.035	0.027	0.034	0.037
(La/Yb)	1.70	6.27	3.18	8.79	3.36	3.22	1.01	1.64	4.09
Rb	662	627	626	514	451	507	1280	774	496
K/Rb	63	65	60	58	84	75	24	46	77
TE_1	1.095	1.06	1.22	1.18	1.10	1.17	1.19	1.17	1.05
TE_3	1.127	1.121	1.12	1.18	1.10	1.02	1.03	1.15	1.02
Method	ICP-AES	ICP-AES	ICP-AES	ICP-AES	ICP-AES	ICP-MS	ICP-MS	ICP-MS	ICP-MS

Table 6. REE contents of separate minerals of the Qianlishan and Baerzhe granites (ppm)

	Qianlishan granite				Baerzhe granite			
	Feldspar	biotite	Topaz	Monanite	Feldspar	Riebeckite	hingganite	Pyrochlore
La	13.9	9.64	68.7	427×10^2	3.86	302	274×10^2	7973
Ce	38.1	27.6	216	866×10^2	13.2	908	130×10^3	294×10^2
Pr	4.02	3.59	30.4	7784	1.74	107	213×10^2	2940
Nd	15.1	14.8	136	169×10^2	6.51	452	839×10^2	7551
Sm	5.86	5.64	54.9	1849	2.28	125	286×10^2	1370
Eu	0.014	0.017	0.04	9.15	0.05	1.38	234	9.3
Gd	6.59	5.80	53.0	1341	2.55	126	257×10^2	976
Tb	1.56	1.20	11.7	109	0.55	21.1	4040	168
Dy	11.1	7.98	73.8	481	3.93	129	197×10^2	1228
Ho	2.09	1.46	12.9	54.6	0.80	23.8	3061	258
Er	6.72	4.43	40.1	451	2.40	59.4	6036	1156
Tm	1.28	0.84	7.43	64.4	0.37	8.00	497	193
Yb	9.34	5.77	51.6	330	2.22	49.4	1889	1571
Lu	1.36	0.87	7.76	48.9	0.30	8.00	190	214
Y	59.4	42.4	327	1952	27.5	817	710×10^2	9605
Σ	171.4	132	1091	160×10^3	68.2	3137	402×10^3	646×10^2
Eu/Eu*	0.007	0.009	0.002	0.027	0.057	0.034	0.028	0.026
$(La/Yb)_N$	1.00	1.13	0.90	73.3	1.17	4.12	9.78	3.42
TE_1	1.17	1.15	1.15	1.33	1.31	1.16	1.51	1.64
TE_3	1.24	1.18	1.24	0.95	1.14	1.05	1.11	1.00
Method	ICP-MS	ICP-MS	ICP-AES	ICP-MS	ICP-MS	ICP-AES	ICP-MS	ICP-AES

ICP-MS: in Guangzhou Institute of Geochemistry, Chinese Academy of Sciences.
ICP-AES: in Central Laboratory of Geological Bureau of Hubei Province.

Table 7. The apparent partition coefficients between the minerals/whole rock in the Qianlishan and Baerzhe granites

	Qianlishan granite				Baerzhe granite				References*		$K_{fluid/melt}$**
	feldspar	biotite	topaz	monazite	microcline	riebeckite	hingganite	pyrochlore	plagioclase	K-feld.	
La	0.34	0.24	1.70	1056	0.04	3.28	298	86.66			
Ce	0.33	0.24	1.86	748	0.05	3.24	464	104.98	0.27	0.044	0.033
Pr	0.23	0.21	1.77	453	0.04	2.75	547	75.39			
Nd	0.23	0.22	2.02	252	0.04	3.03	563	50.65	0.21	0.025	0.032
Sm	0.23	0.22	2.13	72.0	0.04	2.37	540	25.84	0.13	0.018	0.03
Eu	0.47	0.57	1.33	305	0.07	2.03	344	13.68	2.15	1.13	0.07
Gd	0.27	0.23	2.13	54.0	0.04	2.21	451	17.12	0.097	0.11	0.025
Tb	0.29	0.22	2.15	20.1	0.04	1.70	326	13.58			
Dy	0.30	0.22	2.02	13.2	0.05	1.57	240	14.92	0.064	0.006	0.023
Ho	0.33	0.23	2.00	8.51	0.05	1.52	195	16.42			
Er	0.35	0.23	2.11	23.8	0.05	1.25	127	24.30	0.055	0.006	
Tm	0.36	0.24	2.08	18.0	0.05	1.14	71.1	27.59			
Yb	0.38	0.23	2.09	13.3	0.05	1.11	42.6	35.39	0.049	0.012	0.022
Lu	0.37	0.23	2.08	13.2	0.05	1.40	33.3	37.60	0.046	0.006	

**Rhyolitic system, Arth, 1976; Shaw, 1978; Sediments melting, Hanson, 1980.*
***Flynn and Burnham, 1978.*
K-feld. = K-feldspar.

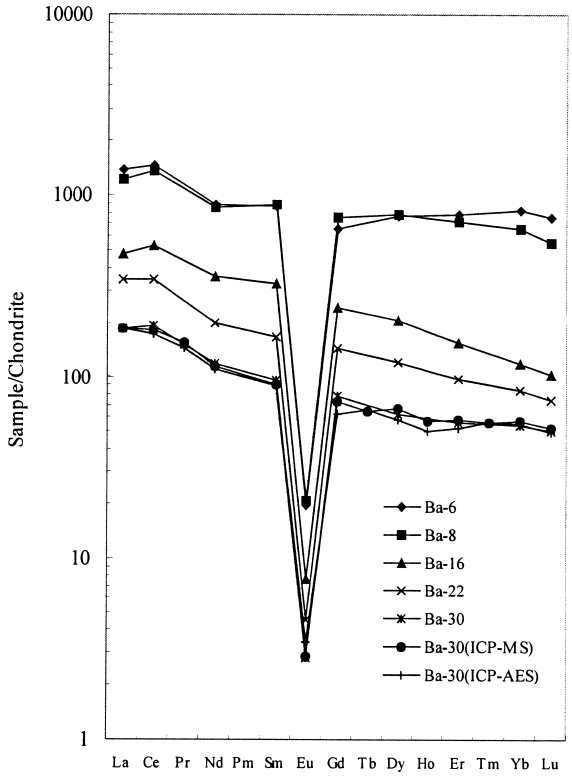

Fig. 7. REE abundance patterns of minerals of the Baerzhe granites analyzed with ID-TIMS. Numbers of the legends are referred to Table 3.

authors (Walker *et al*., 1986; Jolliff *et al*., 1989; Mclennan, 1994) called this type of REE distribution as "kinked REE patterns" resulting from the fractionation of specific minerals. The analyses of apatites from pegmatite have kinked REE patterns and these authors suggested that the REE patterns of these pegmatites could be resulted from fractionation of apatite. Yurimoto *et al*. (1990) modeled the REE variation trend of residual melt and explained the discontinuity between Sm and Nd by monazite fractionation. Our inverstigation demonstrates that rock-forming minerals (feldspar, biotite and riebeckite) and accessory minerals (topaz, monazite, pyrochlore and hingganite) of the Qianlishan and Baerzhe granites possess similar REE tetrad effects and strong Eu depletion with their host rocks (Table 6, Figs. 5 and 6). These characteristic features suggest that the tetrad effect of whole rocks represent the integrated behavior of their constituent minerals. That is, all the individual phases possess the tetrad effect as the melts.

b) The extents of tetrad effect are obviously different among the constituent minerals crystallized from the highly evolved granitic melts rich in alkali and volatiles (Table 6 TE_1, TE_3). The REE-enriched accessory minerals such as monazite, hingganite and pyrochlore are more sensitive to the tetrad effect, especially the first group of REE (La-Nd, TE_1), than those of the other minerals. But, the extents of tetrad effect of the third group of REE (Gd-Ho, TE_3) in the REE-enriched minerals are similar to or slightly lower than those of the feldspar, biotite, riebeckite and topaz in the two granites. These features demonstrate that the contributions to different group of tetrad effect wary among the minerals. The first group of tetrad effect may mainly be controlled by the REE-enriched minerals such as monazite, hingganite and pyrochlore, even though the amounts of these minerals are small in whole-rocks but they are very rich in REE, especially the LREE, as shown by the very high apparent partition coefficients of LREE (Table 7). The total contents of REE ($\sum$REE) of these minerals are very high 160×10^3, 402×10^3, and 646×10^2 ppm respectively, and the $(La/Yb)_N$ ratios representing the enrichment extents of LREE are also high 73.7, 9.78 and 3.42 respectively (Table 6). The rock-forming minerals, such as feldspar, biotite and riebeckite, and volatile-rich topaz all show clearly tetrad effect in all the four groups of REE. The differences of the extents of tetrad effect among the constituent minerals in the two granites hint some characteristic features of the forming process of tetrad effect during the interaction between aqueous fluids and granitic melts. The contributions to the generation of tetrad effect are different among these minerals, for example, the REE, particularly the LREE-enriched minerals strongly influence the generation of the first two groups of REE. Because the melting temperatures of these REE-enriched minerals such as monazite are near the liquidus in granitic systems (Miller and Mittlefehlde, 1982;

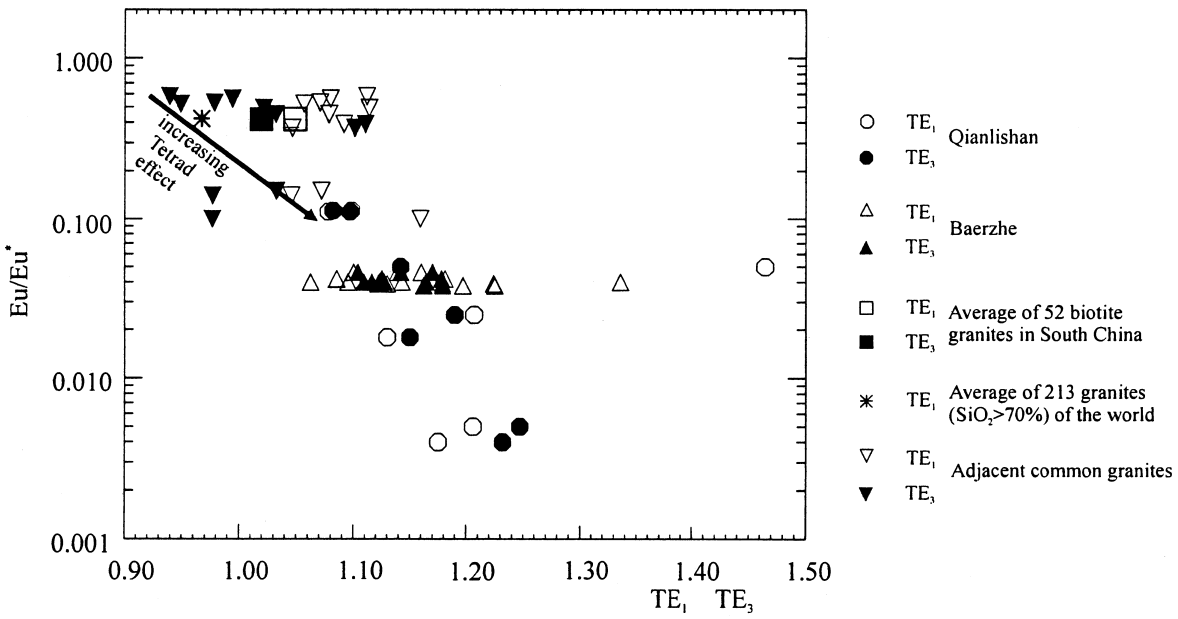

Fig. 8. Tetrad effect (TE_1, TE_3) vs. Eu/Eu in the Qianlishan and Baerzhe granites. The TE_1 and TE_3 are calculated by the formulae of Irber (1999). The data of the average of granites (SGA and WGA) are from Zhao (1992) and Haskin and Haskin (1968).*

Montel, 1986) and their densities are much larger than those of rock-forming minerals. So, the REE-enriched minerals could be crystallized early during the fractional crystallization of the highly evolved granitic melt. The fractionation of these REE-enriched minerals resulted in the tetrad effect of the first two groups of REE. With the increase of the interaction between aqueous fluids and melts, the crystallization of alkali-rich (K, Na) minerals such as feldspars, biotite and riebechite and volatile-rich topaz inherit and progressively promote the tetrad effect of the all four groups of REE.

(3) Granitic melts with REE tetrad effect are highly evolved liquids.

In addition to the identical M-type REE tetrad effect, another common characteristic of whole rocks and their separated minerals of the Qianlishan and Barzhe granites is that they all show strong Eu depletion, which is particularly observed in feldspars. In general Eu is preferentially partitioned into feldspars during crystallization of magma. In previous studies (Arth, 1976; Shaw, 1978; Hanson, 1980) the feldspar/melt Eu partition coefficient was found to be nearly ten times higher than that of other REE, and the Eu/Eu* values of feldspar are higher than or equal to unity in most magmatic systems with clear Eu anomaly (Table 7). The Eu apparent partition coefficients of feldspar in the Qianlishan and Baerzhe granites are higher than other REE (Table 7) but still below 1. In addition a strong Eu negative anomaly exists in feldspar from the Qianlishan and Baerzhe granites, the Eu/Eu* values are 0.007 and 0.057, respectively.

We consider the strong Eu negative anomaly of feldspar to be controlled by the following factors:

a) Granitic melts from which the feidspar and other minerals crystalized in the two granites are strongly depleted in Eu. Namely, the melts are highly evolved and the granites represent the residual liquids which have undergone a high degree of fractional crystallization, mainly of feldspar.

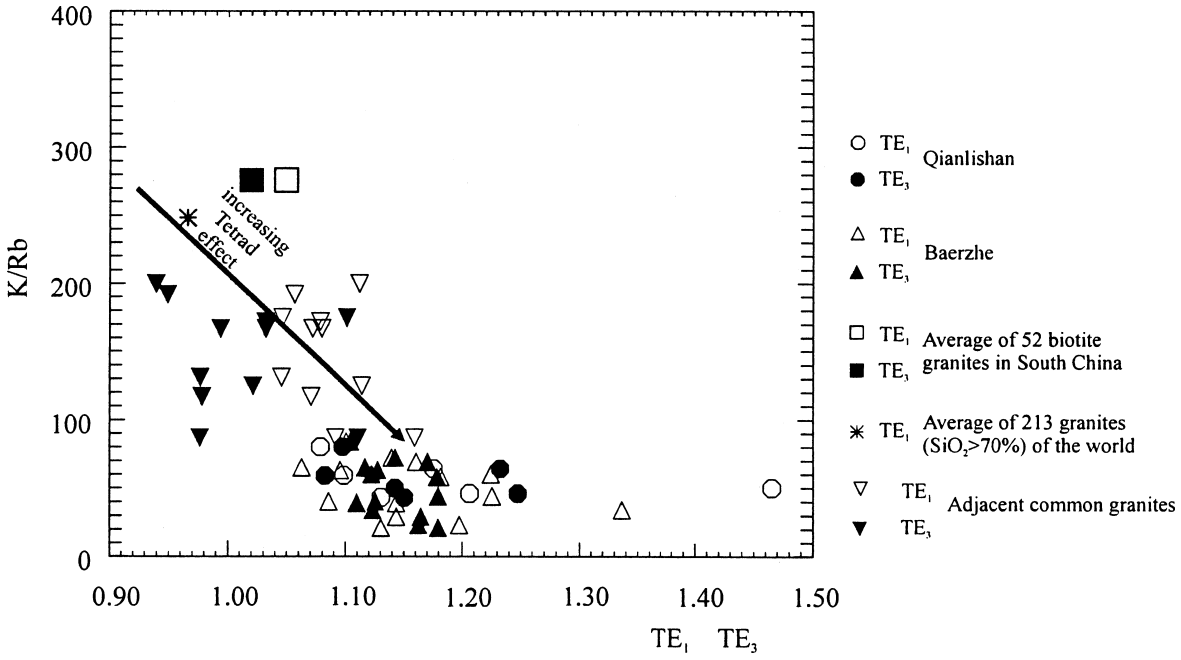

Fig. 9. Tetrad effect (TE_1, TE_3) vs. K/Rb in the Qianlishan and Baerzhe granites.

b) In an experimental system corresponding to a felsic silicate melt and F, Cl-rich fluid (Flynn and Burnham, 1978) Eu was shown to be preferentially partitioned into the fluid phase with other REE. The partition coefficient of Eu between Cl-rich fluid and acidic melt ($K^{Eu}_{flui/mel}$) was found higher than that of the other REE (Table 7) leading to a progressive depletion of Eu in the residual melt. Muecke and Clarke (1981) and Candela (1991) have both proposed that the strong Eu depletion in the late-stage of granite crystallization was attributed to the preferential Eu fractionation into a co-existing Cl-rich aqueous fluid phase rather than into feldspar.

So, the Eu depletion of feldspar in the Qianlishan and Baerzhe granites may show that highly evolved melt and aqueous fluid system or transitional highly evolved melt/aqueous liquids between a silicate melt and an aqueous fluid was co-existing in fractional crystallization of the two granites(see the more discussion below).

On the other hand it can be noted that the tetrad effect is the most clear in the granite samples with the abnormal negative Eu anomalies, such as the Eu/Eu* ratios are even lower than 0.10 in Baerzhe granite (Fig. 8).

(4) Abnormal ratios of trace elements, very high concentration of volatiles such as F and Cl (see above and Table 1) confirm that melts are highly evolved and then an interaction with fluid took place during fractional crystallization of the Qianlishan and Baerzhe granites:

LIL or HFS trace elements ratios such as K/Rb, K/Ba, Rb/Sr, and Zr/Hf which are usually taken as representative of the degree of magma fractionation greatly differ from strongly the average calcium-poor granites in the crust (Turekian and Wedepohl, 1961). The K/Rb ratio is very low (21–90 and 43–64 in the Baerzhe and Qianlishan granites, respectively; 247 in the calcium-poor granites of the crust). The K/Ba ratio is very high (500–2000 and 251–1445 in the Baerzhe and Qianlishan granites, respectively; 50 in the calcium-poor granites of the crust). The Rb/Sr ratio is high and the Zr/Hf ratio is low: the former are 17–38 and 3.4–54.3 in the Baerzhe and Qianlishan granites, respectively, 1.5 in the calcium-poor

granites of the crust; the later are 18–32 and 3.3–22.6 in the Baerzhe and Qianlishan granites, respectively, 44.8 in the calcium-poor granites of the crust.

All of the above abnormal ratios of trace elements show the non-CHARAC (Charge-and-Radius-Controlled) behavior in the Qianlishan and Baerzhe granites. In general the REE tetrad effect is often accompanied by the non-CHARAC behavior. Figure 9 demonstrates the relationship between the tetrad degree (TE_1, TE_3) and the K/Rb ratios. Some adjacent common granites which have not or have very weak REE tetrat effect were plotted for comparision. It is clear that the more decrease of the K/Rb ratios of granites, namely the degree of magma fractionation became the higher, the more pronounced the tetrad effect (Fig. 9).

(5) Fluid/melt interaction is an important factor controlling tetrad effect in granites.

Experiments and investigations have both provided the evidences that the enrichment of highly evolved melts in volatiles and alkaline elements lowers the solidus temperatures of the residual granitic system (Wyllie and Tuttle, 1961; Glyuk and Anfilogov, 1973a, b; Kovalenko, 1978; Manning, 1981; London *et al.*, 1989; Xiong *et al.*, 1999) and eventually leads to the formation of a co-existing magmatic-hydrothermal system (Burnham and Ohomoto, 1980; London, 1986, 1987; London *et al.*, 1989; Thomas, 1994; Irber, 1999; Bau, 1996).That is the highly evolved residual magmatic melts may continuously transfer from melts into high temperature aqueous fluids.This system may be similar to the liquid-liquid extraction system (Peppard *et al.*, 1969). Therefore, a high degree of fractional crystallization and fluid/melt interaction promotes the REE tetrad effect and the strong Eu depletion in residual melt. The rock-forming and accessory minerals inherited the REE bulk composition of the residual melt. Some REE-containing minerals in hydrothermal veins, such as monazite, possess a W-type pattern which counterbalances the M-type tetrad effect (Hong *et al.*, 1999), demonstrating that fluid/melt interaction is the mechanism for the REE tetrad effects in both melt and fluid.

CONCLUSIONS

(1) The REE compositions of the Qianlishan and Barzhe granites were determined using different analytical methods-ICP-AES, ICP-MS and ID-TIMS, and the results consistently show the tetrad effect. The tetrad effect is produced by genuine natural geological and geochemical processes. It is not an artifact due to analytical uncertainties.

(2) Similar M-type REE tetrad effect and strong Eu depletion are observed in whole-rock samples and their constituent minerals in the Qianlishan and Baerzhe granites. Consequently, the tetrad effect represents the integrated behavior of the entire members (=individual phases) of the rocks. The REE tetrad effect is accompanied by strong Eu negative anomalies.

(3) Highly fractional crystallization lead to the enrichment of volatile, alkaline, rare earth elements and rare metals in residual melts which may result in a co-existing magmatic-hydrothermal system. The fluid/melt interaction in this system produces the REE tetrad effect in the melt and in the rock-forming and accessory minerals crystallizing from this melt. The minerals inherited the REE composition and distribution characteristics of the melt. Therefore, the interaction between granitic melt and coexisting volatile-rich fluid is the most important factor controlling the formation of REE tetrad effects in the Qianlishan and Baerzhe granites. This interaction is also responsible for the formation of superlarge W-Bi and polymetallic and REE-Nb-Be-Zr deposits associated with the Qianlishan and Baerzhe granites.

(4) The extents of tetrad effect are different among the constituent minerals of the two granites. During the interaction between aqueous fluids and melts the REE-enriched minerals may mainly controled tetrad effect of the first two groups of REE, the alkali-rich rock-forming and volatile-rich minerals inherit and progressively promot the tetrad effect of the all four groups of REE.

(5) Abnormal ratios of LIL and HFS trace elements in granites can be used as indicators of tetrad effect degree.

(6) The tetrad effect may be used as an important geochemical index or tracer for the petrogenetic evolution and mineralization of granitic magma.

Acknowledgments—The research was funded by National Natural Science Foundation of China No. 49873025, National Climb Project A-30, 95-Yu-25, Major State Basic Research Program of PRC No. 1999043202 and the Chinese Academy of Sciences (grant KZCX2-102).

REFERENCES

Akagi, T., Shabani, M. B. and Masuda, A. (1993) Lanthanide tetrad effect in kimuraite [$CaY_2(CO_3)_4 \cdot 6H_2O$]: Implication for a new geochemical index. *Geochim. Cosmochim. Acta* **57**, 2899–2905.

Arth, J. G. (1976) Behaviour of trace elements during magmatic processes—a summary of theoretical models and their application. *J. Res. USGS* **4**, 1, 41–47.

Bau, M. (1996) Controls on the fractionation of isovalent trace elements in magmatic and aqueous systems: evidence from Y/Ho, Zr/Hf and lanthanide tetrad effect. *Contrib. Mineral. Petrol*. **123**, 323–333.

Boynton, W. V. (1984) Cosmochemistry of the rare earth elements: meteorite studies. *Rare Earth Element Geochemistry. Developments in Geochemistry 2* (Henderson, R., ed.), 89–92, Elsevier, Amsterdam.

Burnham, C. W. and Ohomoto, H. (1980) Late-stage processes of felsic magmatism. *Granitic Magmatism and Related Mineralization* (Ishihara, S. and Takenouchi, S., eds.), *Mining Geology, Special Issue* **8**, 1–11.

Candela, P. A. (1990) Theoretical constraints on the chemistry of magmatic aqueous phase. *Ore-Bearing Granite Systems Petrogenesis and Mineralizing Processes* (Stein, H. J. and Hannah, J. L., eds.), *Geological Society of America, Spec. Pap.* **246**, 11–19.

Flynn, R. T. and Burnham, W. (1978) An experimental determination of rare earth partition coefficients between a chloride containing vapour phase and silicate melts. *Geochim. Cosmochim. Acta* **42**, 685–701.

Frey, F. A. (1984) Rare earth element abundances in upper mantle rocks. *Rare Earth Element Geochemistry* (Henderson, P., ed.), *Developments in Geochemistry* **2**, 153–192.

Glyuk, D. S. and Anfilogov, V. N. (1973a) Phase relation in the system granite-H_2O-HF at a pressure of 1000 kg/cm, *Geochim. Int*. **9**, 321–325.

Glyuk, D. S. and Afilogov, V. N. (1973b) Phase equilibria in the system granite-water-potassium fluoride at a water vapor pressure of 1000 kg/cm. *Dokl. Acad. Sci. USSR, Earth Sci. Sec*. **210**, 237–238.

Govindaraju, K. (1994) Compilations of working values and sample description for 383 geostandards. *Geostandards Newsleter* **18**, Spec. Issue, 1–158.

Hanson, G. N. (1980) Rare earth elements in petrogenetic studies of igneous systems. *Ann. Rev. Earth Planet. Sci*. **4**, 371–406.

Haskin, L. A. and Haskin, M. A. (1968) Rare-earth elements in the Skaergaard intrusion. *Geochim. Cosmochim. Acta* **32**, 433–447.

Henderson, H. (1984) General geochemical properties and abundances of the rare earth elements. *Rare Earth Element Geochemistry* (Henderson, P., ed.), *Develpoments in Geochemistry* **2**, 1–9.

Hidaka, H., Holliger, P., Shimizu, H. and Masuda, A. (1992) Lanthanide tetrad effect observed in the Oklo and ordinary uraninites and its application for their forming processes. *Geochem. J*. **26**, 337–346.

Hong Wenxing, He Songyu, Huang Shunhua, Guo Guozhang, Hou Hongquau and Zhu Xiangkun (1999) Study on the W-type of REE tetrad effect and it's geological significance of the monazites. *Progress in Natural Sciences* **9**, 12 (Suppl.) 1287–1290 (in Chinese).

Irber, W. (1999) The lanthanide tetrad effect and its correlation with K/Rb, Eu/Eu*, Sr/Eu, Y/Ho and Zr/Hf of evolving peraluminous granite suits. *Geochim. Cosmochim. Acta* **63**, 489–508.

Jahn, B. M., Gyuau, G. and Glikson, A. (1982) Komatiites of the overwacht group, S. African: REE geochemistry, Sm/Nd age and mantle evolution. *Contrib. Mineral. Petrol*. **80**, 25–40.

Jolliff, B. L., Papike, J. J. and Shearer, C. K. (1989) Inter-and intro-crystal REE variations in apatite from the Bob Ingersoll Pegmatite, Black Hills, South Dakota. *Geochim. Cosmochim. Acta* **53**, 429–441.

Jørgenson, C. K. (1962) Electron transfer spectra of lanthanide complexes. *Mol. Phys*. **5**, 271–277.

Jørgenson, C. K. (1979) Theoretical chemistry of rare earths. *Handbook on the Physics and Chemistry of Rare Earths*, Vol. 3, 111–169, North-Holland.

Kawabe, I. (1992) Lanthanide tetrad effects in the La^{3+} ionic radii and refined spin-pairing energy theory. *Geochem. J*. **25**, 31–44.

Kovalenko, V. I. (1978) The reactions between granite and aqueous hydrofluoric acid in relation to the origin of fluorine-bearing granites. *Geochem. Int*. **14**, 108–118.

Li, X. H. (1997) Geochemistry of the longsheng

Ophiolite from the southern margin of Yangtze craton, SE China. *Geochem. J.* **31**, 323–337.

Liu, C.-Q., Masuda, A., Okada, A., Yabuki, S., Zhang, J. and Fan, Z. (1993) A geochemical study of loess and desert sand in northern China: Implications for continental crust weathering and composition. *Chem. Geol.* **106**, 359–374.

Liu, Y., Liu, H. and Li, X. H. (1996) Simultaneous and precise determination of 40 trace elements in rock samples using ICP-MS. *Geochemica* **25**, 6, 552–558 (in Chinese with English abstract).

Liu, Y., Dai, T. and Lu, H. Z. (1997) ^{40}Ar-^{39}Ar and Sm-Nd isotopical ages of formation and mineralization of Qianlishan granites. *Sciences in China, D* **27**, 425–430 (in Chinese).

London, D. (1986) Magmatic-hydrothermal transition in the Tanco rare-element pegmatite: evidence from fluid inclusions and phase-equilibrium experiments. *Am. Mineral.* **71**, 376–395.

London, D. (1987) Internal differentiation of rare-element pegmatites: effects of boron, phosphoris, and fluorine. *Geochim. Cosmochim. Acta* **51**, 403–420.

London, D., Morgan, G. B. and Hervig, R. L. (1989) Vapor-undersaturated experiments with Macusani glass + H_2O at 200 Mpa and the internal differentiation of granitic pegmatites. *Contrib. Mineral. Petrol.* **102**, 1–17.

Manning, D. A. C. (1981) The effect of fluorine on liquidus phase relationship in the system Oz-Ab-Or with excess water at 1 kb. *Contrib. Mineral. Petrol.* **76**, 206–215.

Mao, J., Li, H. and Pei, R. (1995) Geology, geochemistry and mineralization of Qianlishan granite. *Mineral Deposits* **14**, I, 12–23 (in Chinese with English abstract).

Masuda, A. and Ikeuchi, Y. (1979) Lanthanide tetrad effect observed in marine environment. *Geochem. J.* **13**, 19–22.

Masuda, A., Kawakami, O., Dohmoto, Y. and Takenaka, T. (1987) Lanthanide tetrad effects in nature: two mutually opposite types, W and M. *Geochem. J.* **21**, 119–124.

Masuda, A., Matsuda, N., Minami, M. and Yamamoto, H. (1994) Approximate estimation of the degree of lanthanide tetrad effect from precise but partially void data measured by isotope dilution and an electron configuration model to explain the tetrad effect phenomenon. *Proc. of Japan Acad. 70, Ser. B* **10**, 169–174.

McLennan, S. M. (1994) Rare earth element geochemistry and the "tetrad" effect. *Geochim. Cosmochim. Acta* **58**, 2025–2033.

Miller, C. F. and Mmittlefehldt, D. F. (1982) Depletion of light rare-earth elements in felsic magmas. *Geology* **10**, 129–133.

Montel, J. M. (1986) Experimental determination of the solubility of Ce-monazite in SiO_2-Al_2O_3-K_2O-Na_2O melts at 800°C, 2 kbar under H_2O-setuated conditions. *Geology* **14**, 659–662.

Muecke, G. K. and Clarke, D. B. (1981) Geochemical evolution of the South Mountain batholith Nova Scotia: Rare-earth element evidence. *Can. Mineral.* **19**, 133–145.

Nugent, L. J. (1970) Theory of the tetrad effect in the lanthanide (III) and actinide (III) series. *J. Inorg. Chem.* **32**, 3485–3491.

Peppard, D. F., Mason, G. W. and Lewey, S. (1969) A tetrad effect in the liquid-liquid extraction ordering of lanthanides (III). *J. Inorg. Nucl. Chem.* **31**, 2271–2272.

Rollinson, H. (1993) *Using Geochemical Data: Evaluation, Presentation, Interpretation*. Longman Scientific Technical, 133–142.

Schilling, J. G. (1975) Rare-earth variations across "normal segments" of the Raykjanes Ridge, 60–53°N, Mid-Atlantic Ridge, 29°S, and East Pacific Rise, 2–19°S, and evidence of the composition of the underlying low-velocity layer. *J. Geophys. Res.* **80**, 1459–1473.

Shaw, D. M. (1978) Trace element behaviour during anatexis in the presence of liquid phase. *Geochim. Cosmochim. Acta* **42**, 7, 933–943.

Siekirerski, S. (1971) The shape of the lanthanide contraction as reflected in the changes of the unit cell volumes, Lanthanide radius and the free energy of complex formation. *J. Inorg. Nucl. Chem.* **33**, 377–386.

Thomas, R. (1994) Fluid evolution in relation to the emplacement of the Variscan granites in the Erzgebirge region: a review of the melts and fluid inclusions evidence. *Metallogeny of Collisional Orogens Focused on the Erzgebirg and Comparable Metallogenic Settings* (Seltmann, R. *et al.*, eds.), 70–81.

Turekian, K. K. and Wedepohl, K. H. (1961) Distribution of the elements in some major units of the earth's crust. *Geol. Soc. Amer. Bull.* **72**, 172–192.

Walker, R. W., Hanson, G. N., Papike, J. J., O'Neil, J. R. and Laul, J. C. (1986) Internal evolution of the Tin Mountain Pegmatite, Black Hills, South Dakota. *Am. Mineral.* **71**, 440–459.

Wang, Y. X. and Zhao, Z. H. (1997) Geochemistry and origin of the Baerzhe REE, Nb, Be, Zr superlarge deposit. *Geochimica* **21**, 24–35 (in Chinese with English abstract).

Wyllie, P. and Tuttle, O. F. (1961) Experimental investigation of silicate systems containing two volatile components. Part II: the effects of NH_3 and HF in

addition to water on the melting temperatures of granite and albite. *Am. J. Sci.* **259**, 128–143.

Xiong, X. L., Zhao, Z. H., Zhu, J. C. and Rao, B. (1999) Phase relations in albite granite-H_2O-HF system and their petrogeneti applications. *Geochem. J.* **33**, 199–214.

Yurimoto, H., Duke, E. F., Opapike, J. J. and Shearer, C. K. (1990) Are discontinuous chondrite-normalized REE patterns in pegmatic granite systems the results of monazite fractionation? *Geochim. Cosmochim. Acta* **54**, 2141–2145.

Zhao, Y. X. (1988) Ore-forming mechanism of Qianlishan granite stock discussed from the relationship of Shizhuyuan W-polymetallic deposit with the stock. *Earth Science* **13**, 2, 155–162 (in Chinese).

Zhao, Z. H. (1988) REE tetrad effects—an important indicator for fluid/melt interaction. *The Proceedings of the 3rd Congress on Mineralogy, Petrology and Geochemistry of China*, 47–49 (in Chinese with English abstract).

Zhao, Z. H. (1992) Petrogenetic models of crust-type and crust-mantle type granitoids as evidenced by REE patterns. *Petrogenesis and Mineralization of Granitoids* (Tu, Guang-zhi, Xu, Keqin and Qiu, Yuzhuo, eds.), 54–65, Science Press, Beijing.

Zhao, Z. H., Masuda, A. and Shabani, M. B. (1992) REE tetrad effects in rare metal granite. *Chinese Journal of Geochemistry* **12**, 221–233.